Electron density distribution in paramagnetic chromium: A γ-ray diffraction study

W. Jauch
Hahn-Meitner-Institut, Glienicker Str. 100, D-14109 Berlin, Germany

M. Reehuis
Max-Planck-Institut für Festkörperforschung, Heisenbergstrasse 1, D-70569 Stuttgart, Germany
(Received 5 October 2005; revised manuscript received 30 November 2005; published 2 February 2006)

High-accuracy single-crystal structure factors, complete up to $\sin\theta/\lambda = 1.78$ Å^{-1} have been measured from paramagnetic chromium at 333 K using 316.5 keV γ radiation. A detailed description of the electron density distribution is derived in terms of a multipolar atomic deformation model. There is pronounced charge asphericity in the valence region arising from preferential occupancy of the t_{2g} subshell. The 3*d* charge distribution is contracted by 12.6% relative to the free atom, in accordance with magnetic synchrotron x ray and neutron measurements. By contrast, the atomic crystal scattering factor deduced from γ-ray diffraction is found to be in contradiction with earlier experimental and theoretical work. Achievement of a reliable Debye-Waller factor is of vital importance in this context. There is no evidence for an anharmonic term in the atomic potential. Real space and energetic features of the charge density topology are used to characterize the directed metallic bonds. Special attention is paid to the form factor approximation in diffraction data analysis.

DOI: 10.1103/PhysRevB.73.085102 PACS number(s): 71.20.Be, 32.80.Cy, 61.10.−i

I. INTRODUCTION

The ground state electron density is the fundamental independent variable of many-electron density-functional theory.[1] Its spatial distribution in the unit cell, $\rho(\mathbf{r})$, is experimentally accessible from high-quality x-ray diffraction data. The diffracted intensities are connected with the structure factors, the Fourier components of $\rho(\mathbf{r})$. The diffraction experiments are demanding since extremely accurate measurements are needed to move from standard crystal structure determination towards addressing the rearrangement of the electron density caused by crystal bonding. In the case of chromium, a number of electron density related studies have appeared in the literature, but these studies are either based on reduced sets of low-order diffraction data or a quantitative representation of the electron density is lacking. It is the purpose of this paper to overcome these limitations, and to deduce an accurate charge density of paramagnetic chromium from an extended set of crystal structure factors by employing γ-ray Bragg diffraction.

With the use of 316.5 keV γ radiation, the high-energy diffraction case (photon energy $\gg K$-shell binding energy) is fully realized making it possible to overcome a number of experimental and theoretical difficulties in the process of deriving structure factors from the observed integrated intensities. It is important to realize that the improvement in accuracy is not only due to the high photon energy but is also brought about by additional favorable experimental conditions, such as the perfect space-time stability of the wide homogeneous incident beam, or the absence of any optical device providing a simple instrumental resolution. The nuclear γ lines have a very narrow spectral spread of $\Delta\lambda/\lambda = 10^{-6}$ so that multiple diffraction is suppressed. It is worth noting that the photon energy used in this work is much beyond 100 keV presently available with synchrotron radiation sources.

Studies of heavier element compounds such as Cr demand a much higher accuracy than studies of organic systems, since the heavier the element, the smaller the fraction of scattering from the valence electrons relative to the core contribution. Furthermore, the small unit cells encountered in highly symmetric elemental solids lead to only few reflections in the low order region where valence scattering is concentrated, calling again for an exceptional accuracy if meaningful information is to be obtained. These handicaps explain the rather limited number of available diffraction data in the case of the transition metals which in view of their importance clearly deserve more experimental attention.

The benefits offered by high-quality γ-ray structure factors data sets have been exploited and realized during the past years in a series of electron density studies on archetype inorganic crystals.[2] Experimental charge densities from simple inorganic materials has been the subject of a recent review.[3] After presenting our results for Cr, a detailed critical assessment of agreement and disagreement will be given with earlier results, deduced from laboratory x ray, synchrotron x ray, electron and neutron diffraction work as well as from *ab initio* band-structure calculations.

II. EXPERIMENTAL AND DATA REDUCTION

Paramagnetic chromium has a body-centered-cubic (bcc) structure (space group $Im\bar{3}m$; $a = 2.8857$ Å at 333 K),[4] in which each atom is surrounded by eight nearest neighbors along the cube diagonals and six next-nearest neighbors along the cube axial directions.

The single crystal used in the present investigation was a cube of dimensions $2.509 \times 2.506 \times 2.500$ mm^3, purchased from MaTecK/Jülich (Germany). Double-crystal γ-ray diffraction with an angular resolution of 1.5″ was used to measure diffraction profiles along three perpendicular directions.

It turned out that the sample consisted of several crystallites, each of them with an isotropic angular full width at half maximum (FWHM) of around 70″.

The diffraction data have been collected on the γ-ray diffractometer installed at the Hahn-Meitner-Institut where the most intense line of an ^{192}Ir source ($T_{1/2}=73.83d$) with a wavelength of 0.0392 Å (316.5 keV) is used. The diffracted γ rays were recorded in ω-step scan mode with an intrinsic germanium detector. The data set, complete up to $\sin\theta/\lambda = 1.78$ Å^{-1}, was collected at 333(1) K, well above the Néel temperature, $T_N=311$ K, so that lowering of symmetry can be excluded as a possible source of interference.

An absorption correction was carried out ($\mu = 0.750$ cm^{-1}),[5] resulting in a transmission range from 0.800 to 0.843. 314 diffraction data were measured corresponding to 79 independent reflections with an unprecedented counting-statistical overall precision of $\Sigma\sigma(I)/\Sigma I=0.0038$ for the averaged data. The absorption-weighted mean path lengths through the sample varied between 2.251 mm and 2.487 mm. It was therefore considered necessary to process each reflection with its individual path length in the calculation of the extinction correction, and to treat symmetrically equivalent reflections separately. Data reduction was carried out using the XTAL suite of crystallographic programs.[6]

The data were corrected for the contribution of inelastic thermal diffuse scattering (TDS) from the acoustic modes to the total intensity. The formalism of Skelton and Katz[7] was applied, using the elastic constants from Bolef and de Klerk[8] and the instrumental parameters defining the sampled volume in reciprocal space: ω-scan peak width=0.7°, full circular detector window=0.46°. The maximum TDS contribution was 16%.

III. RESULTS

Structure refinements were performed with the program system VALRAY,[9] minimizing $\chi^2=\Sigma w(|F_o|^2-|F_c|^2)^2$, where F_o and F_c are the observed and calculated structure factors, respectively. The observations were weighted by their counting-statistical variances.

A. Independent-atom model (IAM)

Cr has the electronic ground state configuration $3d^5 4s$ ($^7S_3$). Scattering factors were calculated from the Hartree-Fock wave functions given in Clementi and Roetti.[10] The fit parameters were the scale factor of the observed structure factors, a secondary extinction parameter using the Becker-Coppens formalism,[11] and the mean square vibrational amplitude. In order to reduce the influence of charge-density deformations in the outer shell, high-order refinements were carried out, taking into account only reflections with $\sin\theta/\lambda > 0.7$ Å^{-1}, not affected by extinction. The resulting scale factor was fixed in later refinements with improved scattering models.

B. Multipole model

In the aspherical atom multipole model the electron density distribution is projected onto a small basis set of nucleus-centered real spherical harmonic functions with the local density rigidly following the motion of its associated nucleus.[12] The atomic density of Cr is represented by three components of the core, $3d$ spherical valence and deformed valence electrons

$$\rho_{Cr}(\mathbf{r}) = \rho_{core}(r) + \kappa^3\rho_{3d}(\kappa r) + P_{hex}\kappa^3\rho_{3d}(\kappa r)K_4(\mathbf{r}/r).$$

For site symmetry $m\bar{3}m$ the lowest nonvanishing higher pole is the Kubic harmonic $K_4(\mathbf{r}/r)$ which is a linear combination of y_{40} and y_{44+}.

The core density is the unperturbed Hartree-Fock (HF) electron density of the appropriate atomic orbitals. The square of the radial part of the $3d$ canonical HF orbitals is used to construct both the monopole and the hexadecapole. The κ parameter allows for expansion ($\kappa<1$) or contraction ($\kappa>1$) of the radial function. A single κ parameter is used for both the spherical valence shell and the deformation function. This constraint is necessary for the subsequent calculation of $3d$ orbital occupancies (see Sec. IV B). P_{hex} is a variable hexadecapole population coefficient. The spherical surface harmonics are expressed relative to a global Cartesian frame which is oriented parallel to the unit cell axes. Several models were examined in the refinement process.

In Table I, the quality of fit is given for the reference scattering models. Further variants will be discussed below. The very high precision of the data is reflected by the large value of χ^2 for the IAM. A large improvement of fit is already obtained with a spherical atom model using the valence-shell radial scaling parameter. The drastic reduction in χ^2 shows that the data strongly supports the multipole model, also to be reflected by the very narrow confidence limits on the fit parameters which are listed in Table II. Note that the normalization condition for the aspherical density function is such that the population coefficients correspond to the local electrostatic moments in Å units.

Since the diffuse $4s$ valence density contributes very little to the scattering, its population cannot be reliably deter-

TABLE I. Quality of fit for the various scattering models based on 314 observations; Np=number of adjustable parameters. In all cases, the scale factor was fixed to the value obtained from a high-order refinement ($\sin\theta/\lambda > 0.7$ Å^{-1}).

	IAM	Monopole	Multipole
χ^2	4797	2542	943
Np	2	3	4

TABLE II. Mean square vibrational amplitude and multipole model parameters of paramagnetic Cr at 333(1) K. Reliability factors for the 314 observations: $R(F)=\Sigma|F_o-F_c|/\Sigma|F_o|=0.0054$, $wR(F^2)=[\Sigma w(F_o^2-F_c^2)^2/\Sigma wF_o^4]^{1/2}=0.0096$.

U (Å^2)	0.00385(1)
κ	1.126(2)
P_{hex} ($\lvert e\rvert$Å^4)	−0.676(37)

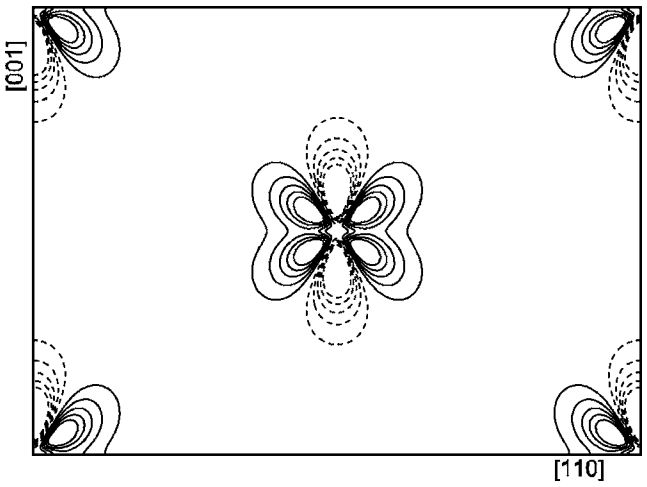

FIG. 1. Aspherical contributions to the static model density in the (110) plane. The density range is from −1.11 to 0.74e Å^{-3}. Solid lines represent regions of excessive density, dashed lines depleted regions in steps of 0.1e Å^{-3}. The zero contour is omitted. The densities are truncated at ±0.5e Å^{-3}.

mined, and is fixed to 1. Tentative omission of 4s resulted only in a minor increase in χ^2.

Adjustment of the secondary extinction parameter gives a Gaussian mosaic width (FWHM) of 67.3(5)″, in perfect agreement with the observed value, convincingly demonstrating that extinction has been treated properly. The maximum reduction of $|F_o|^2$ due to secondary extinction is 21%; a reduction of more than 5% occurs for only three independent reflections.

The positivity of experimental electron densities is not guaranteed by the multipole model. The static model density, with the Debye-Waller factor omitted, was therefore evaluated in direct space; it proved to be positive everywhere in the unit cell. Figure 1 shows the static model deformation density (aspherical components only). The observed features are very pronounced, exhibiting magnitudes up to 1.1e Å^{-3}. The deformation map will be further discussed below.

Transition metal atoms require a multipole expansion at least up to $l=4$. Inclusion of one more symmetry-allowed term in the multipole expansion, y_{60} with a Slater-type radial dependence, leads only to a marginal improvement of the least-squares fit, and is regarded as insignificant.

C. Metallic bond characteristics

According to the atoms-in-molecules (AIM) theory developed by Bader,[13] the interatomic interactions are characterized by local properties at the bond critical saddle points, $\mathbf{r}_c$, of the electron density between two nuclei (two negative perpendicular curvatures and one positive parallel to the bond path). Shared-electron (covalent) interactions have $\nabla^2\rho(\mathbf{r}_c) \ll 0$, typical of charge concentration, whereas closed-shell (ionic) interactions have $\nabla^2\rho(\mathbf{r}_c) \gg 0$, typical of charge depletion. Metallic systems are associated with a flat slowly varying electron density throughout the valence region, and the Laplacian is generally dominated by the positive curvature along the bond path, $\nabla^2\rho(\mathbf{r}_c) > 0$, though all three curvature components may have a small magnitude possibly leading to $\nabla^2\rho(\mathbf{r}_c)$ close to zero (and therefore quite indeterminate). The smaller magnitude of $\nabla^2\rho(\mathbf{r}_c)$ as compared to the strong ionic bond reflects the greater tendency of the charge density to remain in the internuclear region, away from the atomic basins. A quantitative measure of the valence electron density flatness is provided by the ratio $r = \rho_{\min}(\mathbf{r})/\rho_{\max}(\mathbf{r}_c)$, where $\rho_{\min}(\mathbf{r})$ is the absolute minimum of the electron density and $\rho_{\max}(\mathbf{r}_c)$ the maximum density found at a bond critical point.[14] The flatness index r separates metals ($r \to 1$) from nonmetals ($r \to 0$).

Further information about the bonding type is available from the local electron energy densities [$G(\mathbf{r}_c)$=kinetic energy density, $V(\mathbf{r}_c)$=potential energy density, $H(\mathbf{r}_c)=G(\mathbf{r}_c)+V(\mathbf{r}_c)$=total energy density] that can be calculated from $\rho(\mathbf{r}_c)$ and $\nabla^2\rho(\mathbf{r}_c)$ using the approximation for $G(\mathbf{r}_c)$ proposed by Abramov[15] in combination with the local virial theorem from which $V(\mathbf{r}_c)$ can be estimated. For shared-electron interaction, there is a predominance of the (negative) local potential energy, so that $H(\mathbf{r}_c) < 0$, while for closed-shell systems $H(\mathbf{r}_c) \cong 0$ is observed.[2]

Table III summarizes the characteristics of the bond critical points of the static model electron density. There are closed-shell type [$\nabla^2\rho(\mathbf{r}_c) > 0$] bonds between first and second neighbors with the distinguished features of a low electron density and a balance of the kinetic and potential energy densities. The flatness index has the value $r=0.595$, quite remote from the free-electron value of one. The kinetic energy per electron, $G(\mathbf{r}_c)/\rho(\mathbf{r}_c)$, is found to be low (less than one, in atomic units), a property the metallic and the covalent bond have in common.

For a variety of fcc metals, Eberhart *et al.*[16] noticed a linear relationship between bulk modulus and $\nabla^2\rho(\mathbf{r}_c)$, demonstrating that macroscopic elastic behavior correlates with a local property of the charge density. Taking the first neighbor value from Table III [$\nabla^2\rho(\mathbf{r}_c)=0.11$ a.u., bulk modulus $B = 1.901 \times 10^{12}$ dyn/cm^2], the respective proportionality is confirmed also for chromium though it belongs to the different topological bcc familiy.

TABLE III. Characteristics of the bond critical points. $\lambda_\parallel$ denotes the curvature of $\rho(\mathbf{r}_c)$ along the internuclear line (the two negative perpendicular curvatures are degenerate). Values of ρ in eÅ^{-3}, values of $\nabla^2\rho(\mathbf{r}_c)$ and $\lambda_\parallel$ in eÅ^{-5}. G, V, and G/ρ are given in atomic units.

$\mathbf{r}_c$	$\rho(\mathbf{r}_c)$	$\nabla^2\rho(\mathbf{r}_c)$	$\lambda_\parallel$	$G(\mathbf{r}_c)$	$V(\mathbf{r}_c)$	$G(\mathbf{r}_c)/\rho(\mathbf{r}_c)$
$\frac{1}{4}, \frac{1}{4}, \frac{1}{4}$	0.237	2.790(1)	4.03(1)	0.0301(2)	−0.0312(4)	0.858
$\frac{1}{2}, \frac{1}{2}, 0$	0.145	0.926(2)	1.00(1)	0.0112(3)	−0.0127(6)	0.520

IV. DISCUSSION

A. Vibrational parameter

The mean-square amplitude of atomic vibrations is converted from the sample temperature (333 K) to room temperature (295 K) using the linear dependence over the small temperature range, $U(295\ \mathrm{K})=0.00341(1)\ \text{Å}^2$. Neglect of the TDS correction would have resulted in an artificial reduction of U by 7%.

The vibrational parameter obtained in this work is considerably smaller than the value reported by Ohba *et al.*[17] in their x-ray charge density study at 297 K, $U=0.00407(2)\ \text{Å}^2$. The discrepancy is due to the reduced monochromaticity of the graphite monochromated x-ray beam.[18] It contains a bremsstrahlung component with a large wavelength spread that is progressively truncated at higher Bragg angles, inevitably resulting in distorted values for vibrational parameters that are systematically too large. The spectral width of the 316.5 keV photon beam is $\Delta\lambda/\lambda=10^{-6}$ and no monochromator is needed.

Several other experimental methods have been used in the determination of the chromium vibrational parameter at ambient temperature. From measurement of x-ray high-order powder reflections at two temperatures, $U=0.00344(8)\ \text{Å}^2$ was obtained.[19] The values, $0.00337\ \text{Å}^2$ and $0.00331\ \text{Å}^2$, were calculated by Peljo[20] from a lattice dynamical model based on the results of inelastic neutron scattering measurements by Shaw and Muhlestein[21] and Feldman,[22] respectively. Refinement of an extended single crystal neutron diffraction data set ($\sin\theta/\lambda \leqslant 1.5\ \text{Å}^{-1}$) gave $U=0.00337(4)\ \text{Å}^2$.[23] There is thus excellent agreement between the independent estimates of U.

The possible influence of anharmonic contributions to the Debye-Waller factor has also been investigated. For $m\bar{3}m$ point symmetry there can be no third-order modifications but there is one isotropic and one anisotropic quartic term in the Gram-Charlier expansion of the atomic probability density function. Combined multipole-anharmonicity refinement leads only to an insignificant improvement of fit. There is thus no noticeable anharmonic component in the atomic potential, and the harmonic approximation has to be considered as adequate. Our result is supported by x-ray single crystal diffraction[17] but disagrees with an x-ray powder study.[20] According to this study, the independently-vibrating atom potential should show an isotropic softening which would imply a larger thermal displacement than in a harmonic potential. The reported room-temperature value, $0.00315(11)\ \text{Å}^2$, is inconsistent with the values presented above.

An adequate description of thermal motion is a necessary condition for a meaningful extraction of charge density information from the diffraction data. Validation of the thermal parameter is therefore an important issue lending support and credibility to the further conclusions.

B. *d* orbital populations

The $3d$ electron density of a transition metal atom may be described by spherical harmonic functions or, alternatively, it may be expressed in terms of the orbital components of its atomic wave function. By equating the two descriptions of the density, a set of linear equations is obtained from which the orbital occupancies can be derived from the multipole populations ($l_{\max}=4$).[24] With an octahedral environment, the d orbitals split into doublet e_g and triplet t_{2g} orbitals. In a bcc metal, the t_{2g} orbitals point towards the nearest neighbors while e_g is directed towards the second nearest neighbors.

From the refined multipole parameters follows 66.4(2)% t_{2g} and 33.6(2)% e_g for the $3d^5$ configuration. The population of the t_{2g} orbitals is thus significantly larger than 60%, the value for a spherical charge distribution. The orbital occupancies are clearly reflected in the deformation map (Fig. 1) where the dominant features are electron buildup along $\langle 111\rangle$, pointing towards the nearest neighbors, and electron depletion towards the second nearest neighbors. The experimental charge asphericity of Cr metal displayed by Ohba *et al.*[17] is quite different from Fig. 1: whereas charge accumulation is qualitatively reproduced, the corresponding depletion along $\langle 100\rangle$ is practically missing. The number of d electrons which contribute to the aspherical charge density is given as $Z_a=n(t_{2g})-\frac{3}{2}n(e_g)$, with n indicating the number of electrons having symmetry t_{2g} or e_g; the deduced value is $Z_a=0.80(1)$.

In the bcc metals there occur pairs of reflections such as (330/411), (431/510) at identical values of $\sin\theta/\lambda$, which would have the same intensity if the charge density were spherically symmetric. From measurement of a couple of such reflections, the t_{2g} population in Cr was estimated to be 67.0(2.3)%;[25] in an earlier study[26] about 72% (no standard deviation is given) was found. There is thus agreement on the asphericity of the charge distribution, with the present work providing a substantial advance in accuracy.

C. Form factors

1. X-ray form factor

For the radial scaling parameter, κ, a very pronounced deviation from the IAM is observed. The $3d^5$ valence shell exhibits a spatial contraction of 12.6%, which corresponds to a form factor expansion relative to the free atom. The atomic form factor f_{hkl} is related to the fitted structure factor F_{hkl} through $f_{hkl}=F_{hkl}/2$, so that for a monatomic crystal the static values are simply obtained by multiplication with the inverse Debye-Waller factor. The structure factor contains a contribution from nuclear Thomson scattering, $f_N=(Ze)^2/Mc^2$. For chromium, $f_N=0.0061$ electron units, which is accounted for. Absolute values of the atomic crystal scattering factor for the first 16 diffraction vectors are listed in Table IV, where also the numerical contributions of both the core and valence electrons have been individually identified. Our experimentally derived values are now compared with earlier x ray and electron diffraction measurements, performed on an absolute scale.

Cooper's[27,28] work on a powder sample using Ag-Kα radiation gave a scattering factor (corrected for anomalous dispersion) that for the first six reflections was about 5% lower than the theoretical free-atom value. The observed values of f at higher $\sin\theta/\lambda$ are already too low due to an overesti-

TABLE IV. Static scattering factors from the multipole model fit for chromium in units of e/atom. f_{core} and f_{valence} denote the contributions from the core and $3d^5$ valence electrons, respectively. f is the total contribution from all electrons. f_{IAM} is calculated from Ref. 10, and f_{theory} is taken from Ref. 33.

hkl	$\sin\theta/\lambda(\text{Å}^{-1})$	f_{core}	f_{valence}	f	f/f_{IAM}	f/f_{theory}
110	0.2451	14.618	2.475	17.093	1.021	1.049
200	0.3466	12.464	1.407	13.871	1.020	1.036
211	0.4245	10.983	0.925	11.908	1.024	1.021
220	0.4902	9.931	0.609	10.540	1.022	1.014
310	0.5481	9.164	0.355	9.519	1.014	1.013
222	0.6004	8.588	0.302	8.890	1.020	1.008
321	0.6485	8.143	0.182	8.325	1.015	1.007
400	0.6932	7.790	0.033	7.823	1.002	1.008
330	0.7353	7.502	0.072	7.574	1.011	1.005
411	0.7353	7.502	0.022	7.524	1.004	1.006
420	0.7751	7.260	0.009	7.269	1.005	1.005
332	0.8129	7.051	0.036	7.087	1.010	1.004
422	0.8490	6.867	−0.003	6.864	1.006	1.004
431	0.8837	6.701	−0.016	6.685	1.005	1.004
510	0.8837	6.701	−0.080	6.621	0.995	1.005
521	0.9493	6.408	−0.062	6.346	0.999	1.003

mated vibrational parameter [U=0.00374 Å^2].[28] It seems also possible that the sample suffered from some chemical change, probably oxidation, since Hosoya[29] noticed a gradual decrease with time of Cr powder intensities for measurements in open air, which ceased for a protected sample.

Later, single-crystal experiments were performed on a plate of 0.05 mm thickness.[26] The integrated intensities of a few low-order reflections, obtained at different spots from the crystal surface, were plotted as a function of the square of the reciprocal half-width, a relationship chosen because it gave the best linear trend line. Extrapolation to infinite half-width resulted in a crystal form factor, after correcting for anomalous dispersion, up to 6% smaller than free-atom theory, so that an expansion of the 3d charge distribution was inferred. Contrary to Cooper's data, however, the difference between the two types of scattering factor diminishes with increasing $\sin\theta/\lambda$. The following objections may be raised against the thin-plate technique: (i) the extrapolation procedure lacks theoretical justification, and (ii) it is susceptible to systematic errors arising from residual primary and secondary extinction, and surface irregularities which always decrease the measured intensity. In the context of secondary extinction, the pitfalls of phenomenological extrapolation to establish a zero-extinction limit have been revealed by one of the authors.[30]

High-energy electron diffraction allows determination of the scattering factor for a first-order reflection by exploiting a dynamical scattering effect. Owing to destructive interference, the intensity of the second-order reflection will show a minimum at a particular electron accelerating voltage known as the critical voltage. The first-order value is determined from the measured voltage by many-beam calculations covering higher-order Fourier coefficients. Knowledge of the Debye-Waller factor is essential. Furthermore, it is assumed that the higher-order terms can be described in the independent-atom approximation. From room temperature measurements, two x-ray scattering factors have been determined, f_{110} and f_{200}, which are 2.5% and 1% smaller than those for free atoms.[31,32] An important source of error appears to be in the second-order structure factors which are definitely affected by bonding effects (see Table IV). Though the precision of a critical-voltage experiment may be very high, the accuracy in structure factor determination depends upon other measured and calculated values.

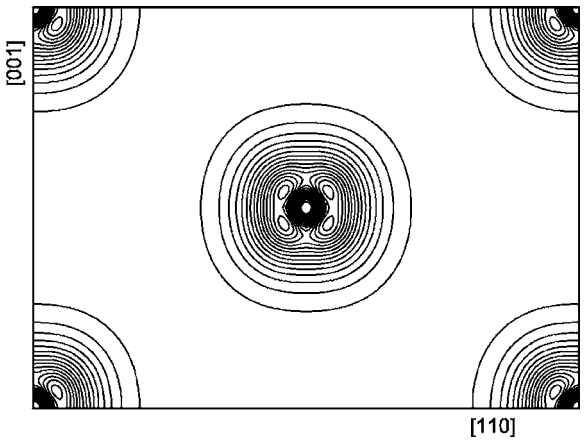

FIG. 2. Static model valence density in the (110) plane. Contours are drawn at intervals of 0.5e Å^{-3}.

A comprehensive band-structure calculation for paramagnetic chromium was performed by Laurent *et al.*,[33] who employed the self-consistent linear combination of Gaussian orbitals method, and used the computed wave functions also to determine the x-ray form factor, tabulated up to $\sin\theta/\lambda$ =0.95 Å^{-1}. In Table IV, it is shown that the three lowest-order values are 5.0–2.2 % smaller than the model fit values, while the deviation for the higher orders smoothly approaches 0.5% or less. The observed disagreement between theory and experiment therefore cannot be attributed to an inadequate experimental scaling factor. Rather, it is an indication that the d orbitals have a radial extension different from the predicted one. The charge density is more concentrated around the nuclei.

A further *ab initio* calculation[17] was based upon the augmented plane wave method, and a valence electron density map as well as the x-ray form factor have been reported. The theoretical map compares very well with the present model valence density which is depicted in Fig. 2. In the experimental map, peaks of 7.75e Å^{-3} are found on the ⟨111⟩ axes at 0.20 Å from the Cr nucleus. The corresponding theoretical values are 5.8e Å^{-3} and 0.23 Å. At a deeper quantitative level, however, the low order Fourier coefficients are again smaller than the model fit values by up to 5.1%. As core and valence contributions have been given individually, the source of discrepancy between theory and experiment can be identified unambiguously. There is perfect agreement concerning the inner electrons, whereas the theoretical valence form factors appear to be systematically reduced in the order of 50%.

The comparison has shown up difficulties and discrepancies. The results from the literature share one common feature, that is, an apparent expansion of the valence charge distribution is found. On the other hand, the γ-ray data require an opposite behavior, namely, a large contraction of the valence shell which supports the conjecture by O'Keeffe *et al.*[34] that, as a general rule, the valence-electron density should be contracted in monatomic crystals. This hypothesis is based on measurements of the average electrostatic potential using electron-beam techniques, eventually contradicting the often-reported expansion of the valence shell in crystalline silicon.

2. Magnetic form factor

Complementary information about the spatial extent of the d electrons can be obtained from magnetic form factor measurements. While in neutron diffraction only the total magnetic moment is accessible, proportional to the sum $L+2S$ of the orbital and spin angular momentum, high-energy magnetic x-ray diffraction is sensitive to the ordered spin component only. Synchrotron radiation at 100 keV was used to measure several points of the magnetic form factor.[35] A pure spin nature of the ordered-moment was inferred by Moon *et al.*[36] from a neutron diffraction investigation of antiferromagnetic chromium. Both the neutron and the x-ray data are in excellent agreement, substantiating the presence of a pure spin moment and the quenching of the orbital contribution. The results could be well described by the spherical atomic form factor for the $3d^4 4s^2$ configuration. Similarly, polarized neutron studies of the field-induced magnetic moment distribution have been interpreted in terms of $3d^4 4s^2$.[37] It should be noted, however, that this configuration represents an excited state. Its shape is practically indistinguishable from the ground state scattering factor ($3d^5 4s^1$) with an associated expansion of 12.6% in scattering space (see Table IV). The radial density contraction found in the present paramagnetic study is thus quantitatively corroborated. The spherical contraction should be invariant with respect to the magnetic phase, as has indeed been observed in the case of the transition-metal monoxides.[2] It is important to realize that interpretation of the magnetic form factors was invariably based on literature values from 1961 (Table 4 in Ref. 38), when an accurate ground state wave function for Cr was not yet available, and for this reason, an absence of solid-state effects has been incorrectly concluded.

3. Localized versus diffuse d electrons

The electron density analysis, discussed so far, is based on a localized atomic model of the electron density in the crystal. In simple metals, the valence electrons, originating from s- and p-type orbitals, are itinerant and do not contribute to the Bragg intensities, so that the scattering factors should be smaller than those for free atoms. This is not the case with transition metals, such as Cr (see Table III), where the bonding involves d states which are much more localized, and where the Fermi surface lacks any resemblance to the free-electron sphere. Concerns expressed by Ohba *et al.*[17] that for a metallic state an accurate scale factor may not be obtainable from neutral atom scattering factors are thus invalidated.

In a recent study[39] of metallic bonding in Cu ($3d^{10}4s^1$), the $3d$ radial density was written as $3d_{\mathrm{crystal}}=3d^{10-n}4s^n$ to account for partial delocalization, and it was found that a $3d$ function from Cu^{+2} and $4s$ from neutral atom produced by far the best fit with the surprisingly large value at $n=1.27(6)$. An electron transfer from $3d$ to $4sp$ of this order is at variance with the diamagnetism and the absence of any aspherical charge deformation in Cu, so that a strong physical interpretation of n has to be abandoned. A more reserved interpretation suggests the occurrence of a diffuse $3d$ density, closely resembling $3d^9$ due to the reduced screening effect of the partially delocalized electrons.

Jiang *et al.*[39] proposed that this model of delocalization should also be useful for the transition metals, and so we have applied it to chromium. Writing $3d_{\mathrm{crystal}}=3d^{5-n}4s^n$ with the $3d$ function from Cr^{+2} yields $n=0.92(12)$, and the same quality of fit as the neutral atom model. The extra parameter n thus turns out to be irrelevant, effectively mimicking the electron count of the underlying d shell model. It should further be pointed out that the $4s$ part in the $3d_{\mathrm{crystal}}$ radial function acts as a formal electroneutrality constraint being otherwise inconsequential in view of its vanishing scattering contribution. No explanation can be offered why in the Cu study the introduction of n leads to the amazing improvement in R factor by an order of magnitude. To conclude, there is no indication for a failure of the localized electron model in chromium.

4. Relativistic form factors

The atomic form factors of the charge distribution are the most important theoretical components used to analyze and interpret the diffraction data. A better approximation to the exact elastic (Rayleigh) scattering amplitudes than the ordinary form factor $f(q)$ is the modified relativistic form factor $g(q)$, introduced first by Franz,[40] which takes into account electron binding effects.[41] It is no longer the Fourier transform of the charge distribution as in the classical form factor approximation. For an atomic electron with wave function ψ, it takes the form $g(q)=\int|\psi(r)|^2 e^{\mathrm{iqr}} f(r) d\tau$, with $f(r)=[1-|\varepsilon|+|V(r)|]^{-1}$, where ε is the electron binding energy and $V(r)$ is the electrostatic potential (both in units of mc^2). The choice $f(r)=1$ corresponds to the form factor approximation. The modified form factor is found by summing over all electrons in the atom. Its size for $q=0$ is reduced from the atomic number Z, the sum rule result for free electrons at rest, to $g(0)=Z-|E_0|/mc^2$ where E_0 is the total ground-state binding energy. The reduction is a consequence of the relativistic mass increase of deeper core electrons which decreases their response to the external electromagnetic field. For Cr, the reduction in the effective number of electrons is 0.055. A complete evaluation of total atom and K-shell values of $g(q)$ has been given by Schaupp *et al.*[42] for all elements. The reduced K-shell values must not be confused with an apparent radial core expansion. One should also not be misled by the impression that the relevance of $g(q)$ is restricted to high energies. Rather, the relativistic reduction in scattering power is independent of the energy of the scattered x rays.

An important feature to be noted is that $f(q)$ based on nonrelativistic wave functions comes closer to $g(q)$ than the ordinary form factor obtained from relativistic wave functions. For chromium at $\sin\theta/\lambda=1$ Å^{-1}, the relativistic correction $\Delta=g-f$ amounts to -0.03 and -0.06 e/atom when referred to nonrelativistic and relativistic $f(q)$, respectively, which corresponds to a relative deviation of 0.5% and 1%. The relativistic $f(q)$ thus overestimates the effect of relativity in the atom since the reduction from binding is neglected, that is, relativity is included only incompletely.

It has been recommended to apply the relativistic corrections to the experimental data,[43] and improved results have seemingly arrived at.[44] In practice, such a procedure requires independent information on scale and thermal parameters, and even then, its feasibility is limited to monatomic structures. As having made clear above, Δ is not uniquely defined, but only relative to a theoretical IAM reference $f(q)$, and therefore bears no direct relation to the measurements, so that the transfer of a theoretical deficiency to the observational data must be considered with reservation. An acceptable alternative is to include Δ in the scattering factor model, acting as a real-valued x-ray dispersion term. This seems to be a sufficiently good approximation since both quantities are largely independent of $\sin\theta/\lambda$, being primarily due to the inner electrons of the atom. The refined parameter values obtained in this way were not statistically different from those in Table II, as to be expected from an effect essentially due to a 1.5% reduction of the K-shell nonrelativistic $f(q)$.

Though deviations from the form factor approximation pose an interpretative problem in high accuracy work, in particular for heavier elements, its gravity should not be overestimated. Note that the occurrence of a relativistic reduction is not confined to x-ray scattering but is shared in all applications, e.g. electron diffraction, which rely on a simple Fourier transform relation between scattering amplitude and target distribution, a framework which holds in nonrelativistic scattering theories but not in relativity. Whereas a great deal of effort has been invested over the years on improved wave functions in the calculation of $f(q)$, much less attention has been paid to formalisms going beyond the form factor approximation.

V. CONCLUDING REMARKS

An extended set of high-quality structure factors, achieved by the use of 316.5 keV γ radiation, has provided the currently best possible representation of the electron distribution in Cr. Important findings include the following: (i) validation of data quality and scale factor estimate by comparison with available values of the thermal vibrational parameter; (ii) anharmonic thermal motion is negligible; (iii) the $3d$-shell exhibits a spherical contraction of $12.6\pm0.2\%$; (iv) excess occupation of the t_{2g} orbitals towards the nearest neighbors, accompanied by depletion of e_g density towards the second neighbors; (v) directional metallic bonding features are quantitatively characterized in terms of electron density properties; (vi) no indication for a failure of the localized $3d$ electron model is detected. Finally, it should be emphasized that the high accuracy of the present method serves as a sensitive and useful test of *ab initio* calculations, with the revealed deviations underlining the need to improve the level of accuracy in the theoretical predictions.

ACKNOWLEDGMENT

We are pleased to acknowledge helpful and stimulating discussions with Dr. H.-J. Bleif.

[1] P. Hohenberg and W. Kohn, Phys. Rev. **136**, B864 (1964).
[2] W. Jauch, Acta Crystallogr., Sect. A: Found. Crystallogr. **A60**, 264 (2004); W. Jauch and M. Reehuis, Acta Crystallogr., Sect. A: Found. Crystallogr. **A61**, 411 (2005).
[3] J. M. Zuo, Rep. Prog. Phys. **67**, 2053 (2004).
[4] M. E. Straumanis and C. C. Weng, Acta Crystallogr. **8**, 367 (1955).
[5] J. H. Hubbell and S. M. Seltzer, National Institute of Standards and Technology Internal Report No. 5632 (1995). Also available via http://www.physics.nist.gov/PhysRefData/XrayMassCoef/cover.html.
[6] Computer code XTAL 3.4, *User's Manual*, edited by S. R. Hall, G. S. D. King, and J. M. Stewart (University of Western Ausralia, Perth, Australia, 1995).
[7] E. F. Skelton and J. L. Katz, Acta Crystallogr., Sect. A: Cryst. Phys., Diffr., Theor. Gen. Crystallogr. **A25**, 319 (1969).
[8] D. I. Bolef and J. de Klerk, Phys. Rev. **129**, 1063 (1963).
[9] R. F. Stewart, M. Spackman, and C. Flensburg, computer code VALRAY, *User's Manual* (Carnegie-Mellon University, Pittsburgh, Pennsylvania, and University of Copenhagen, Copenhagen, Denmark, 2000).
[10] E. Clementi and C. Roetti, At. Data Nucl. Data Tables **14**, 177 (1974).
[11] P. J. Becker and P. Coppens, Acta Crystallogr., Sect. A: Cryst. Phys., Diffr., Theor. Gen. Crystallogr. **A31**, 417 (1975).
[12] R. F. Stewart, Acta Crystallogr., Sect. A: Cryst. Phys., Diffr., Theor. Gen. Crystallogr. **A32**, 565 (1976).
[13] R. F. W. Bader, *Atoms in Molecules: A Quantum Theory* (Clarendon, Oxford, 1990).
[14] P. Mori-Sánchez, A. Martín Pendás, and V. Luaña, J. Am. Chem. Soc. **124**, 14721 (2002).
[15] Yu. A. Abramov, Acta Crystallogr., Sect. A: Found. Crystallogr. **A53**, 264 (1997).
[16] M. E. Eberhart, M. M. Donovan, and R. A. Outlaw, Phys. Rev. B **46**, 12744 (1992).
[17] S. Ohba, Y. Saito, and S. Wakoh, Acta Crystallogr., Sect. A: Cryst. Phys., Diffr., Theor. Gen. Crystallogr. **A38**, 103 (1982).
[18] B. Rousseau, S. T. Maes, and A. T. H. Lenstra, Acta Crystallogr., Sect. A: Found. Crystallogr. **A56**, 300 (2000).
[19] T. Paakkari, Acta Crystallogr., Sect. A: Cryst. Phys., Diffr., Theor. Gen. Crystallogr. **A30**, 83 (1974).
[20] E. Peljo, Phys. Scr. **26**, 103 (1982).

[21] W. M. Shaw and L. D. Muhlestein, Phys. Rev. B **4**, 969 (1971).
[22] J. L. Feldman, Phys. Rev. B **1**, 448 (1970).
[23] J. Strempfer, Th. Brückel, G. J. McIntyre, F. Tasset, Th. Zeiske, K. Burger, and W. Prandl, Physica B **267-268**, 56 (1999).
[24] A. Holladay, P. Leung, and P. Coppens, Acta Crystallogr., Sect. A: Cryst. Phys., Diffr., Theor. Gen. Crystallogr. **A38**, 563 (1982).
[25] S. Ohba and Y. Saito, Acta Crystallogr., Sect. A: Cryst. Phys., Diffr., Theor. Gen. Crystallogr. **A38**, 725 (1982).
[26] M. Diana and G. Mazzone, Phys. Rev. B **5**, 3832 (1972).
[27] M. J. Cooper, Philos. Mag. **7**, 2059 (1962).
[28] M. J. Cooper, Philos. Mag. **10**, 177 (1964).
[29] S. Hosoya, J. Phys. Soc. Jpn. **19**, 235 (1964).
[30] W. Jauch and A. Palmer, Acta Crystallogr., Sect. A: Found. Crystallogr. **A58**, 448 (2002).
[31] O. Terasaki, Y. Uchida, and D. Watanabe, J. Phys. Soc. Jpn. **39**, 1277 (1975).
[32] A. G. Fox, Philos. Mag. B **45**, 275 (1993).
[33] D. G. Laurent, J. Callaway, J. L. Fry, and N. E. Brener, Phys. Rev. B **23**, 4977 (1981).
[34] M. O'Keeffe and J. C. H. Spence, Acta Crystallogr., Sect. A: Found. Crystallogr. **A50**, 33 (1994).
[35] J. Strempfer, Th. Brückel, W. Caliebe, A. Vernes, H. Ebert, W. Prandl, and J. R. Schneider, Eur. Phys. J. B **14**, 63 (2000).
[36] R. M. Moon, W. C. Koehler, and A. L. Trego, J. Appl. Phys. **37**, 1036 (1966).
[37] C. Stassis, G. R. Kline, and S. K. Sinha, Phys. Rev. Lett. **31**, 1498 (1973).
[38] A. J. Freeman and R. E. Watson, Acta Crystallogr. **14**, 231 (1961).
[39] B. Jiang, J. Friis, R. Holmestad, J. M. Zuo, M. O'Keeffe, and J. C. H. Spence, Phys. Rev. B **69**, 245110 (2004).
[40] W. Franz, Z. Phys. **98**, 314 (1936).
[41] L. Kissel, B. Zhou, S. C. Roy, S. K. S. Gupta, and R. H. Pratt, Acta Crystallogr., Sect. A: Found. Crystallogr. **A51**, 271 (1995).
[42] D. Schaupp, M. Schmacher, F. Smend, and P. Rullhusen, J. Phys. Chem. Ref. Data **12**, 467 (1983).
[43] R. A. Bonham, in *Electron and Magnetization Densities in Molecules and Crystals*, edited by P. Becker (Plenum Press, New York, 1980).
[44] C. Petrillo, F. Sacchetti, and G. Mazzone, Acta Crystallogr., Sect. A: Found. Crystallogr. **A54**, 468 (1998).